donic acid drives postnatal neurogenesis and elicits a beneficial effect on prepulse inhibition, a biological trait of psychiatric illnesses, PLoS One 4 (2009) e5085.
[20] A. Malandrini, F. Mari, S. Palmeri, S. Gambelli, G. Berti, M. Bruttini, A.M. Bardelli, K. Williamson, V. van Heyningen, A. Renieri, PAX6 mutation in a family with aniridia, congenital ptosis, and mental retardation, Clin. Genet. 60 (2001) 151–154.
[21] M.T. Mercadante, R.M. Cysneiros, J.S. Schwartzman, R.M. Arida, E.A. Cavalheiro, F.A. Scorza, Neurogenesis in the amygdala: a new etiologic hypothesis of autism? Med. Hypotheses 70 (2008) 352–357.
[22] I. Mikkola, J.A. Bruun, T. Holm, T. Johansen, Superactivation of Pax6-mediated transactivation from paired domain-binding sites by dna-independent recruitment of different homeodomain proteins, J. Biol. Chem. 276 (2001) 4109–4118.
[23] T.N. Mitchell, S.L. Free, K.A. Williamson, J.M. Stevens, A.J. Churchill, I.M. Hanson, S.D. Shorvon, A.T. Moore, V. van Heyningen, S.M. Sisodiya, Polymicrogyria and absence of pineal gland due to PAX6 mutation, Ann. Neurol. 53 (2003) 658–663.
[24] E.M. Morrow, S.Y. Yoo, S.W. Flavell, T.K. Kim, Y. Lin, R.S. Hill, N.M. Mukaddes, S. Balkhy, G. Gascon, A. Hashmi, S. Al-Saad, J. Ware, R.M. Joseph, R. Greenblatt, D. Gleason, J.A. Ertelt, K.A. Apse, A. Bodell, J.N. Partlow, B. Barry, H. Yao, K. Markianos, R.J. Ferland, M.E. Greenberg, C.A. Walsh, Identifying autism loci and genes by tracing recent shared ancestry, Science 321 (2008) 218–223.
[25] N. Osumi, The role of Pax6 in brain patterning, Tohoku J. Exp. Med. 193 (2001) 163–174.
[26] J. Prosser, V. van Heyningen, PAX6 mutations reviewed, Hum. Mutat. 11 (1998) 93–108.
[27] K. Ranade, M.S. Chang, C.T. Ting, D. Pei, C.F. Hsiao, M. Olivier, R. Pesich, J. Hebert, Y.D. Chen, V.J. Dzau, D. Curb, R. Olshen, N. Risch, D.R. Cox, D. Botstein, High-throughput genotyping with single nucleotide polymorphisms, Genome Res. 11 (2001) 1262–1268.
[28] R. Scardigli, N. Baumer, P. Gruss, F. Guillemot, I. Le Roux, Direct and concentration-dependent regulation of the proneural gene Neurogenin2 by Pax6, Development 130 (2003) 3269–3281.
[29] E.K. Schorry, M. Keddache, N. Lanphear, J.H. Rubinstein, S. Srodulski, D. Fletcher, R.I. Blough-Pfau, G.A. Grabowski, Genotype-phenotype correlations in Rubinstein–Taybi syndrome, Am. J. Med. Genet. A 146A (2008) 2512–2519.
[30] S.M. Sisodiya, S.L. Free, K.A. Williamson, T.N. Mitchell, C. Willis, J.M. Stevens, B.E. Kendall, S.D. Shorvon, I.M. Hanson, A.T. Moore, V. van Heyningen, PAX6 haploinsufficiency causes cerebral malformation and olfactory dysfunction in humans, Nat. Genet. 28 (2001) 214–216.
[31] S. Sukumar, S. Wang, K. Hoang, C.M. Vanchiere, K. England, R. Fick, B. Pagon, K.S. Reddy, Subtle overlapping deletions in the terminal region of chromosome 6q24.2-q26: three cases studied using FISH, Am. J. Med. Genet. 87 (1999) 17–22.
[32] B.H. Ticho, C. Hilchie-Schmidt, R.T. Egel, E.I. Traboulsi, R.J. Howarth, D. Robinson, Ocular findings in Gillespie-like syndrome: association with a new PAX6 mutation, Ophthalmic Genet. 27 (2006) 145–149.
[33] T. Tominaga, W. Meng, K. Togashi, H. Urano, A.S. Alberts, M. Tominaga, The Rho GTPase effector protein, mDia, inhibits the DNA binding ability of the transcription factor Pax6 and changes the pattern of neurite extension in cerebellar granule cells through its binding to Pax6, J. Biol. Chem. 277 (2002) 47686–47691.
[34] C.C. Ton, H. Hirvonen, H. Miwa, M.M. Weil, P. Monaghan, T. Jordan, V. van Heyningen, N.D. Hastie, H. Meijers-Heijboer, M. Drechsler, B. Royer-Pokora, F. Collins, A. Swaroop, L.C. Strong, G.F. Saunders, Positional cloning and characterization of a paired box- and homeobox-containing gene from the aniridia region, Cell 67 (1991) 1059–1074.
[35] I. Tzoulaki, I.M. White, I.M. Hanson, PAX6 mutations: genotype-phenotype correlations, BMC Genet. 6 (2005) 27.
[36] V. van Heyningen, K.A. Williamson, PAX6 in sensory development, Hum. Mol. Genet. 11 (2002) 1161–1167.
[37] J.H. Wen, Y.Y. Chen, S.J. Song, J. Ding, Y. Gao, Q.K. Hu, R.P. Feng, Y.Z. Liu, G.C. Ren, C.Y. Zhang, T.P. Hong, X. Gao, L.S. Li, Paired box 6 (PAX6) regulates glucose metabolism via proinsulin processing mediated by prohormone convertase 1/3 (PC1/3), Diabetologia 52 (2009) 504–513.
[38] H.E. Xu, M.A. Rould, W. Xu, J.A. Epstein, R.L. Maas, C.O. Pabo, Crystal structure of the human Pax6 paired domain-DNA complex reveals specific roles for the linker region and carboxy-terminal subdomain in DNA binding, Genes Dev. 13 (1999) 1263–1275.

Jpn J Ophthalmol 2009;53:7–11
DOI 10.1007/s10384-008-0619-6

CLINICAL INVESTIGATION

Central Corneal Thickness in Japanese Children

Akiko Hikoya[1], Miho Sato[1], Kinnichi Tsuzuki[2], Yuka Maruyama Koide[1], Ryo Asaoka[1], and Yoshihiro Hotta[1]

[1] Department of Ophthalmology, Hamamatsu University School of Medicine, Hamamatsu, Japan; [2] Department of Ophthalmology, Aichi Children's Health and Medical Center, Obu, Japan

Abstract

Purpose: To determine the central corneal thickness (CCT) in Japanese children and to investigate the changes in CCT with increasing age.

Methods: Pachymetry was performed on 338 eyes of 169 patients undergoing eye muscle surgery under general anesthesia, and the intraocular pressure (IOP) was measured on 312 eyes of 156 of those same patients. Patients with abnormalities other than refractive errors and strabismus were excluded. Patients were divided into four groups: group 1, ≤1 year of age; group 2, 2–4; group 3, 5–9; and group 4, 10–18 years of age. Analysis of variance (ANOVA) was performed to determine the significance of the changes in CCT.

Results: The average CCT of the right eye was 544.3 ± 36.9 μm. The CCT was thinner in group 1 than in groups 3 and 4 (ANOVA, $P = 0.02$). There was a positive but weak correlation between IOP and CCT (IOP = 6.253 + 0.014 × CCT; $r^2 = 0.047$, $P = 0.007$).

Conclusions: CCT reaches the adult thickness in Japanese children by age 5 years. The average CCT is thinner in Japanese children than in Caucasians but thicker than in African American children. **Jpn J Ophthalmol** 2009;53:7–11 © Japanese Ophthalmological Society 2009

Key Words: central corneal thickness, child, general anesthesia, intraocular pressure, ultrasound pachymeter

Introduction

Measuring central corneal thickness (CCT) has become increasingly important, particularly for the diagnosis and management of glaucoma. The Ocular Hypertension Treatment Study reported that subjects with ocular hypertension had greater CCT,[1] and subjects with smaller CCT had a higher risk of developing glaucoma.[2]

Goldmann applanation tonometer measurement is based on the assumption that CCT is 500 μm, a thickness obtained from measurements of cadaver eyes. Because a permanent thinning or flattening of the cornea induces lower intraocular pressure (IOP) after refractive surgery,[3,4] special attention has been paid to the variability of CCT in the healthy population and in patients with various eye diseases. To obtain an accurate IOP value, measurements with the Goldmann applanation tonometer should be corrected by the CCT value.[5] Thus, measuring CCT has become essential for determining true IOP for glaucoma management.

Children with congenital glaucoma also have significantly thinner CCT than healthy children.[6,7] However, aphakic[8,9] and pseudophakic[10] children with glaucoma have significantly thicker CCT than healthy children. These findings then raise the question of why up to 45% of aphakic children who have thicker than average CCT develop glaucoma.[11] Muir et al.[12] speculated that CCT increases after cataract surgery because of endothelial cell damage, or because increased IOP injures the endothelial cells. Thus, measuring CCT in children who are at high risk for glaucoma, such as children with aphakic or pseudophakic eyes, is important.

Received: January 25, 2008 / Accepted: September 26, 2008
Correspondence and reprint requests to: Miho Sato, Department of Ophthalmology, Hamamatsu University School of Medicine, 1-20-1 Handa-yama, Higashi-ku, Hamamatsu 431-3192, Japan
e-mail: mihosato@hama-med.ac.jp

Another important factor that influences the CCT is race or ethnicity. The CCT of African American adults is thinner than that of Caucasian adults,[2,13] and lower IOP in African Americans may delay the diagnosis of glaucoma and determination of an appropriate treatment target.[14] CCT in the Japanese population has been found to be thinner than in Chinese and Filipino populations.[15]

These racial differences are also found in the pediatric population. African American children have thinner CCT than do Caucasian[16] or Hispanic children.[17] A literature search on PubMed did not extract any CCT data regarding healthy Japanese children. Knowing the normal range of CCT of Japanese children is important for diagnosing and treating pediatric glaucoma.

Thus, the purpose of this study was to determine the CCT in Japanese children and to investigate the changes in CCT with increasing age. To accomplish this, we measured the CCT of 338 eyes of 169 children ≤18 years of age by ultrasound pachymetry under general anesthesia.

Subjects and Methods

All patients scheduled for strabismus surgery under general anesthesia were recruited from Hamamatsu University School of Medicine and Aichi Children's Health and Medical Center from December 2005 to August 2007. Patients with corneal disease, a history of intraocular surgery, glaucoma, cataract, or eyelid abnormalities were excluded. Patients known to have abnormally thin corneas such as those with Down syndrome[18] or with Marfan syndrome,[19] or abnormally thick corneas such as those with aniridia,[20] were also excluded.

This study was approved by the Institutional Review Board of the Hamamatsu University School of Medicine and Aichi Children's Health and Medical Center. Full explanation of the research, including the measurement procedures for CCT and IOP was given, and written informed consent was obtained from a parent or legal guardian of each of the patients.

For controls, we measured the CCT of eight healthy subjects aged 26 to 52 years under topical anesthesia.

CCT was measured between 9:00 and 16:00 in the operating room with an ultrasound pachymeter (SP-100 Handy, 1640 Hz; Tomey, Nagoya, Japan). Measurements started within 5 min of endotracheal intubation. All patients were sedated by inhalation or intravenously, and a muscle relaxant was given before insertion of the airway tube. Sevoflurane and nitrous oxide were used to maintain surgical anesthesia during the surgery. The patient's eyelid was held open manually, with special care taken not to press on the eye. One drop of topical anesthesia (4% oxybuprocaine) was administered, and the central cornea was defined as the center of the pupil. The pachymeter probe was placed perpendicularly on the center of the cornea, and the average of eight measurements was recorded as the CCT. Next, the IOP was measured with a Tono-Pen XL (Reichert, Depew, NY, USA). All measurements were performed first on the right eye and then on the left eye.

For statistical purposes, only the data from the right eye were used. The patients were divided into four groups: group 1, ≤1 year of age; group 2, 2–4; group 3, 5–9; and group 4, 10–18 years of age. Statistical analysis was performed using StatView version J-5.0 for Windows (SAS Institute, Cary, NC, USA). Analysis of variance (ANOVA) with a Bonferroni post hoc test was used to determine the significance of any differences among the age groups. Paired *t* tests were used for comparisons between eyes. Linear regression was used to determine the correlation between CCT and IOP. A P value of <0.05 was considered to be statistically significant.

Results

We measured the CCT of 338 eyes of 169 subjects (87 boys, 82 girls) with a mean age of 6.01 ± 3.87 years and an age range of 8 months to 18 years. The patient age distribution and the IOP and CCT measurements are summarized in Table 1.

The average CCT of the right eye was 544.3 ± 36.9 μm (range, 429–648 μm). The CCT distribution is shown in Fig. 1. The CCT was significantly different between age groups (ANOVA $P = 0.0198$); it was significantly thinner in group 1 than in groups 3 or 4 ($P = 0.0071$ and 0.0157, respectively, Bonferroni; Table 1). The average CCT in group 4 was 550.6 μm, which was not significantly different from the mean CCT of the eight healthy adult subjects (525–586 μm).

Table 1. Subjects' characteristics and measurement of CCT and IOP

	n (%)	CCT (μm)	IOP (mmHg)
All patients	169 (100)		
Age distribution (years)		(right eye)	(right eye)
0–1	14 (8)	522 ± 26.7	14.07 ± 2.89
2–4	50 (30)	538 ± 36.6 *	14.14 ± 2.55
5–9	77 (45)	550 ± 36.7 **	14.13 ± 2.13
10–18	28 (17)	550 ± 37.5	12.88 ± 2.45

Values are means ± SD.
CCT, central corneal thickness; IOP, intraocular pressure.
*$P = 0.0071$.
**$P = 0.0157$.

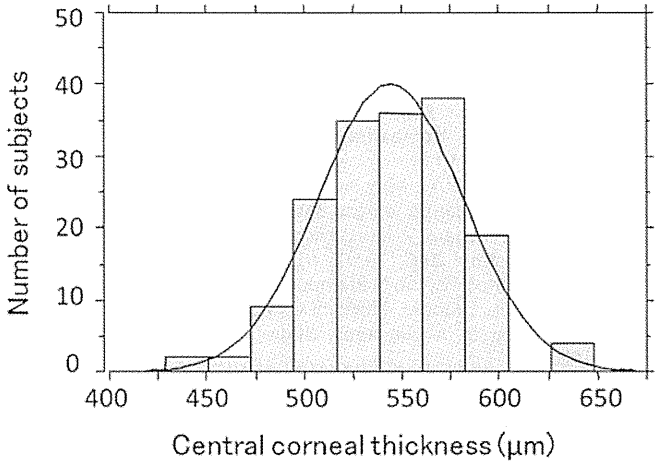

Figure 1. Distribution of central corneal thickness (CCT) in the right eye of children aged 0 to 18 years. CCT is normally distributed. The average CCT was 544.3 ± 36.9 μm.

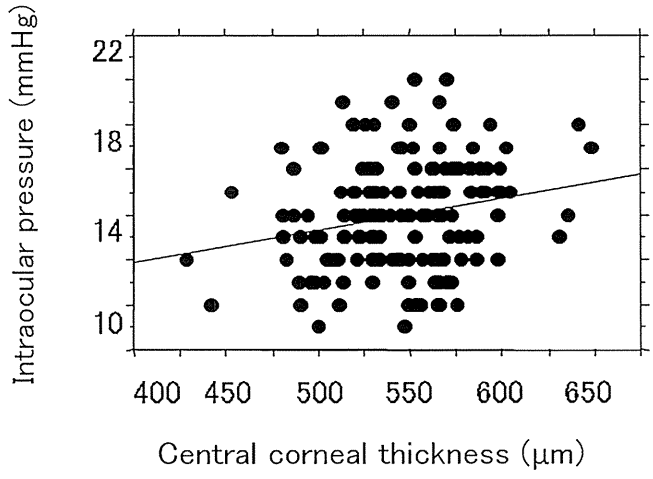

Figure 2. Relationship between CCT and intraocular pressure (IOP). There is a positive but weak correlation between CCT and IOP.

The mean CCT in our adults was comparable to the published average range for the adult Japanese population.[21,22]

The average IOP in the right eye was 13.9 ± 2.4 mmHg (range, 9.0–10.0 mmHg). The IOP did not differ significantly among the different age groups. IOP (y) and CCT (x) were positively correlated, but the correlation coefficient was low ($y = 6.253 + 0.014x$, $r^2 = 0.047$; $P = 0.007$; Fig. 2).

Discussion

Differences in CCT values measured with different instruments have been reported,[23–25] but the values obtained by ultrasound pachymetry and by noncontact optical low-coherence reflectometry are reported to be highly correlated.[26] Bovelle et al.[27] reported that the Topcon specular microscope gives significantly lower values than the ultrasound pachymeter. Suzuki et al.[21] compared CCT values obtained using Orbscan scanning-slit corneal topography/pachymetry, the Topcon SP-2000P, noncontact specular microscopy, and Tomey ultrasonic pachymetry in a Japanese population. The mean CCT was not significantly different between scanning-slit topography (546.9 ± 35.4 μm) and ultrasonic pachymetry (548.1 ± 33.0 μm). However, contact specular microscopy gave a significantly smaller mean (525.3 ± 31.4 μm) than did the other two instruments.[21] Therefore, it is advisable not to compare CCT values obtained using different instruments.

Table 2. Comparison of CCT values of children by race

Race	Hussein[29] (μm)	Dai[17] (μm)	This study (μm)
Caucasians	551	563	
Hispanic	550	568	
Japanese			544
African Americans	532	523	

The SP100 ultrasonic pachymeter is compact and easy to use in the operating room. The measurements are accurate if the instrument is used appropriately. We took special care to place the probe on the center of the cornea because the cornea is thinnest at the center.[28,29]

In adults, CCT is negatively correlated with age in men,[30] or in both sexes.[31] In children, CCT is reported to decrease rapidly during the neonatal period,[32,33] and then to increase slowly and reach the adult level at 3[34] or 5 years of age.[29] Sawa[35] studied the Japanese population and found that the mean CCT of 1-month-old infants (534 ± 36 μm) is thicker than that of 3-month-old infants (508 ± 22 μm), but they found no difference between the 3-month-old infants and the 20- to 29-year-old adults (516 ± 17 μm). Muir et al.[36] suggested that CCT slowly increases in children up to the age of 5 and then decreases at around age 10–14 years. Hussein et al.[29] reported that CCT increases in children until age 9 years and then decreases between ages 10 and 14.[29] In our study, CCT was significantly less in group 1 than in groups 3 or 4, suggesting that adult CCT values are reached by 5 years of age.

Earlier studies have reported racial differences in CCT, not only in adults but also in children. Table 2 summarizes results from other countries for CCTs in pediatric populations from 0 to 18 years of age, measured with ultrasound pachymetry. We understand that it is not ideal to compare our data directly with those of previous reports, but as long as all the measurements were obtained with ultrasound pachymetry, it is reasonable to do so. Compared with the readings obtained from two different institutions,[17,29] the CCT of Japanese children still appears to be thicker than that of African American children and thinner than that of Caucasian or Hispanic children.

Studies focusing on the relationship between CCT and IOP have reported a significant correlation between IOP and CCT in children,[36] as in adults. Suzuki et al.[31] studied Japanese adults and found that IOP measured with the

Jpn J Ophthalmol
Vol 53: 7–11, 2009

Goldmann applanation tonometer was positively correlated with CCT. We found a positive correlation between CCT and IOP measured by Tono-Pen in children, but the correlation coefficient was low.

The Tono-Pen is generally used in children whose IOP is neither very high (>21 mmHg) nor very low (<9 mmHg).[37] IOPs obtained with Tono-Pen are significantly correlated with those obtained using the Goldmann tonotmeter.[38,39] IOPs measured with the Goldmann tonometer, the noncontact tonometer, and the Tono-Pen are known to be influenced by CCT, but IOPs measured by Tono-Pen are less affected by CCT than the other tonometers.[40,41]

We are aware that measured IOP differs significantly with the type and state of anesthesia; for example, succinylcholine can increase IOP, whereas halothane can reduce it.[42] In addition, IOP in the human infant depends strongly on the level of relaxation.[42]

In conclusion, the CCT of Japanese children increases up to age 5 years, when it does not differ significantly from that of adults. The CCT of Japanese children is thinner than that of Caucasian children but thicker than that of African American children. Knowing the average CCT value in the Japanese pediatric population will be useful when caring for not only congenital anomalies involving the cornea but also pediatric glaucoma.

References

1. Brandt JD, Beiser JA, Kass MA, Gordon MO. Central corneal thickness in the Ocular Hypertension Treatment Study (OHTS). Ophthalmology 2001;108:1779–1788.
2. Gordon MO, Beiser JA, Brandt JD, et al. The Ocular Hypertension Treatment Study: baseline factors that predict the onset of primary open-angle glaucoma. Arch Ophthalmol 2002;120:714–720; discussion 829–830.
3. Chatterjee A, Shah S, Bessant DA, et al. Reduction in intraocular pressure after excimer laser photorefractive keratectomy. Correlation with pretreatment myopia. Ophthalmology 1997;104: 355–359.
4. Mardelli PG, Piebenga LW, Whitacre MM, Siegmund KD. The effect of excimer laser photorefractive keratectomy on intraocular pressure measurements using the Goldmann applanation tonometer. Ophthalmology 1997;104:945–948; discussion 9.
5. Ehlers N, Bramsen T, Sperling S. Applanation tonometry and central corneal thickness. Acta Ophthalmol (Copenh) 1975;53: 34–43.
6. Henriques MJ, Vessani RM, Reis FA, et al. Corneal thickness in congenital glaucoma. J Glaucoma 2004;13:185–188.
7. Wygnanski-Jaffe T, Barequet IS. Central corneal thickness in congenital glaucoma. Cornea 2006;25:923–925.
8. Simon JW, O'Malley MR, Gandham SB, et al. Central corneal thickness and glaucoma in aphakic and pseudophakic children. J AAPOS 2005;9:326–329.
9. Tai TY, Mills MD, Beck AD, et al. Central corneal thickness and corneal diameter in patients with childhood glaucoma. J Glaucoma 2006;15:524–528.
10. Simsek T, Mutluay AH, Elgin U, et al. Glaucoma and increased central corneal thickness in aphakic and pseudophakic patients after congenital cataract surgery. Br J Ophthalmol 2006;90:1103–1106.
11. Kirwan C, O'Keefe M. Paediatric aphakic glaucoma. Acta Ophthalmol Scand 2006;84:734–739.
12. Muir KW, Duncan L, Enyedi LB, et al. Central corneal thickness: congenital cataracts and aphakia. Am J Ophthalmol 2007;144:502–506.
13. La Rosa FA, Gross RL, Orengo-Nania S. Central corneal thickness of Caucasians and African Americans in glaucomatous and nonglaucomatous populations. Arch Ophthalmol 2001;119:23–27.
14. Shimmyo M, Ross AJ, Moy A, Mostafavi R. Intraocular pressure, Goldmann applanation tension, corneal thickness, and corneal curvature in Caucasians, Asians, Hispanics, and African Americans. Am J Ophthalmol 2003;136:603–613.
15. Aghaian E, Choe JE, Lin S, Stamper RL. Central corneal thickness of Caucasians, Chinese, Hispanics, Filipinos, African Americans, and Japanese in a glaucoma clinic. Ophthalmology 2004;111: 2211–2219.
16. Muir KW, Duncan L, Enyedi LB, Freedman SF. Central corneal thickness in children: Racial differences (black vs. white) and correlation with measured intraocular pressure. J Glaucoma 2006;15:520–523.
17. Dai E, Gunderson CA. Pediatric central corneal thickness variation among major ethnic populations. J AAPOS 2006;10:22–25.
18. Evereklioglu C, Yilmaz K, Bekir NA. Decreased central corneal thickness in children with Down syndrome. J Pediatr Ophthalmol Strabismus 2002;39:274–277.
19. Sultan G, Baudouin C, Auzerie O, et al. Cornea in Marfan disease: Orbscan and in vivo confocal microscopy analysis. Invest Ophthalmol Vis Sci 2002;43:1757–1764.
20. Brandt JD, Casuso LA, Budenz DL. Markedly increased central corneal thickness: an unrecognized finding in congenital aniridia. Am J Ophthalmol 2004;137:348–350.
21. Suzuki S, Oshika T, Oki K, et al. Corneal thickness measurements: scanning-slit corneal topography and noncontact specular microscopy versus ultrasonic pachymetry. J Cataract Refract Surg 2003; 29:1313–1318.
22. Wu LL, Suzuki Y, Ideta R, Araie M. Central corneal thickness of normal tension glaucoma patients in Japan. Jpn J Ophthalmol 2000;44:643–647.
23. Thomas J, Wang J, Rollins AM, Sturm J. Comparison of corneal thickness measured with optical coherence tomography, ultrasonic pachymetry, and a scanning slit method. J Refract Surg 2006;22: 671–678.
24. Kim HY, Budenz DL, Lee PS, et al. Comparison of central corneal thickness using anterior segment optical coherence tomography vs ultrasound pachymetry. Am J Ophthalmol 2008;145:228–232.
25. Mishima S. Corneal thickness. Surv Ophthalmol 1968;13:57–96.
26. Airiani S, Trokel SL, Lee SM, Braunstein RE. Evaluating central corneal thickness measurements with noncontact optical low-coherence reflectometry and contact ultrasound pachymetry. Am J Ophthalmol 2006;142:164–165.
27. Bovelle R, Kaufman SC, Thompson HW, Hamano H. Corneal thickness measurements with the Topcon SP-2000P specular microscope and an ultrasound pachymeter. Arch Ophthalmol 1999;117:868–870.
28. Remon L, Cristobal JA, Castillo J, et al. Central and peripheral corneal thickness in full-term newborns by ultrasonic pachymetry. Invest Ophthalmol Vis Sci 1992;33:3080–3083.
29. Hussein MA, Paysse EA, Bell NP, et al. Corneal thickness in children. Am J Ophthalmol 2004;138:744–748.
30. Nomura H, Ando F, Niino N, et al. The relationship between age and intraocular pressure in a Japanese population: the influence of central corneal thickness. Curr Eye Res 2002;24:81–85.
31. Suzuki S, Suzuki Y, Iwase A, Araie M. Corneal thickness in an ophthalmologically normal Japanese population. Ophthalmology 2005;112:1327–1336.
32. Autzen T, Bjornstrom L. Central corneal thickness in full-term newborns. Acta Ophthalmol (Copenh) 1989;67:719–720.
33. Autzen T, Bjornstrom L. Central corneal thickness in premature babies. Acta Ophthalmol (Copenh) 1991;69:251–252.
34. Ehlers N, Sorensen T, Bramsen T, Poulsen EH. Central corneal thickness in newborns and children. Acta Ophthalmol (Copenh) 1976;54:285–290.

35. Sawa M. Measurement of corneal thickness. Jap Rev Clin Ophthalmol (Ganka Rinsho Iho) 1986;80:177–184.
36. Muir KW, Jin J, Freedman SF. Central corneal thickness and its relationship to intraocular pressure in children. Ophthalmology 2004;111:2220–2223.
37. Kao SF, Lichter PR, Bergstrom TJ, et al. Clinical comparison of the Oculab Tono-Pen to the Goldmann applanation tonometer. Ophthalmology 1987;94:1541–1544.
38. Bordon AF, Katsumi O, Hirose T. Tonometry in pediatric patients: a comparative study among Tono-pen, Perkins, and Schiotz tonometers. J Pediatr Ophthalmol Strabismus 1995;32:373–377.
39. Dohadwala AA, Munger R, Damji KF. Positive correlation between Tono-Pen intraocular pressure and central corneal thickness. Ophthalmology 1998;105:1849–1854.
40. Bhan A, Browning AC, Shah S, et al. Effect of corneal thickness on intraocular pressure measurements with the pneumotonometer, Goldmann applanation tonometer, and Tono-Pen. Invest Ophthalmol Vis Sci 2002;43:1389–1392.
41. Yildirim N, Sahin A, Basmak H, Bal C. Effect of central corneal thickness and radius of the corneal curvature on intraocular pressure measured with the Tono-Pen and noncontact tonometer in healthy schoolchildren. J Pediatr Ophthalmol Strabismus 2007;44: 216–222.
42. Dominguez A, Banos S, Alvarez G, et al. Intraocular pressure measurement in infants under general anesthesia. Am J Ophthalmol 1974;78:110–116.

Subfoveal Choroidal Thickness after Treatment of Central Serous Chorioretinopathy

Ichiro Maruko, MD,[1] Tomohiro Iida, MD,[1] Yukinori Sugano, MD,[1] Akira Ojima, MD,[1] Masashi Ogasawara, MD,[1] Richard F. Spaide, MD[2]

Purpose: To evaluate the subfoveal choroidal thickness after treatment of central serous chorioretinopathy (CSC) visualized by enhanced depth imaging spectral-domain optical coherence tomography (EDI OCT) and indocyanine green angiography (ICGA).

Design: Retrospective, comparative series.

Participants: Twenty patients (20 eyes).

Methods: The subfoveal choroidal thickness and height of the serous retinal detachment before and after treatment was measured using EDI OCT. Areas of choroidal vascular hyperpermeability were visualized with ICGA. Eyes with classic CSC were treated with laser photocoagulation (LP), whereas eyes with chronic CSC, which are not amenable to LP, were treated with half-dose verteporfin photodynamic therapy (PDT).

Main Outcome Measures: Change in choroidal thickness and height of the serous retinal detachment after treatment.

Results: There were 12 eyes in the LP group and 8 eyes in the PDT group. The serous subretinal fluid resolved in both groups after treatment. In the LP group, the mean choroidal thickness was 345±127 μm at baseline and 340±124 μm at 4 weeks, a difference that was not significant ($P = 0.2$). The mean choroidal thickness in the PDT group increased significantly from 389±106 μm at baseline to 462±124 μm ($P = 0.008$) by 2 days after treatment, and then reduced rapidly to 360±100 μm ($P = 0.001$) at 1 week and 330±103 μm ($P<0.001$) after 4 weeks as compared with baseline. Indocyanine green angiography showed decreased hyperpermeability in the PDT group after treatment.

Conclusions: The subretinal fluid resolved in both disease groups; however, the choroidal thickness and hyperpermeability seen during ICGA was reduced after PDT. These findings suggest that PDT reduces the choroidal vascular hyperpermeability seen in CSC and may work by a different mechanism than LP.

Financial Disclosure(s): The author(s) have no proprietary or commercial interest in any materials discussed in this article. *Ophthalmology 2010;117:1792–1799*

Central serous chorioretinopathy (CSC) is characterized by an idiopathic serous retinal detachment in the posterior pole associated with 1 or more leaks from the level of the retinal pigment epithelium (RPE).[1] Gass[2] proposed that choriocapillaris hyperpermeability was the cause of CSC, and later studies found multifocal areas of choroidal vascular hyperpermeability in CSC patients during indocyanine green angiography (ICGA).[1,3–7] Some patients with CSC have a recent onset of disease with 1 or only a few specific points of leakage from the RPE; these cases are commonly termed *classic CSC*. Other patients with chronic disease have broad areas of granular hyperfluorescence during fluorescein angiography associated with many indistinct areas of leakage. These patients have chronic CSC, which also has been called *diffuse retinal pigment epitheliopathy*.[1,8]

Although some cases of CSC may resolve spontaneously, treatment may be required in eyes with persistent leakage. Laser photocoagulation (LP) typically is used in classic CSC, but is ineffective in chronic CSC.[1,9,10] Photodynamic therapy (PDT) with verteporfin causes resolution of leakage and consequently of the subretinal fluid in both classic and chronic forms of CSC.[11–14] A possible mechanism of action of PDT in CSC involves damage to the choriocapillaris leading to decreased choroidal vascular hyperpermeability and consequently a reduction in leakage from the level of the RPE.

Optical coherence tomography (OCT) uses short coherence length interferometry to image tissue in vivo, particularly the posterior pole of the eye. Conventional OCT has a limited ability to image the choroid because of scattering by pigment within the RPE and by pigment and blood in the choroid and because of a depth-dependent roll-off in sensitivity of spectral-domain OCT instruments in general.[15] A method to improve imaging of the choroid was developed, enhanced depth imaging (EDI) OCT,[15] and by using this technique, the choroid in eyes with CSC was found to be much thicker than normal.[16] The current study evaluated the potential changes in choroidal thickness after treatment of both classic CSC using LP and chronic CSC using half-dose verteporfin PDT. These findings may help to elucidate the pathophysiologic features of CSC as well as its response to treatment.

ISSN 0161-6420/10/$–see front matter
doi:10.1016/j.ophtha.2010.01.023

Table 1. The Clinical Changes of the Mean Choroidal Thickness and the Mean Height of Serous Retinal Detachment during the Follow-up Periods in the Laser Photocoagulation and the Photodynamic Therapy Groups

Case No.	Age (yrs)	Gender	Best-Corrected Visual Acuity (Logarithm of the Minimum Angle of Resolution)		Choroidal Thickness (μm)				Height of Serous Retinal Detachment (μm)			
			Baseline	*Final*	*Baseline*	*Day 2*	*Week 1*	*Week 4*	*Baseline*	*Day 2*	*Week 1*	*Week 4*
Laser photocoagulation												
1	46	F	0.9 (0.05)	1.0 (0.0)	213		205	210	313		221	41
2	51	M	1.2 (−0.08)	1.2 (−0.08)	605		614	585	229		345	124
3	38	M	0.9 (0.05)	0.9 (0.05)	423		436	396	134		103	26
4	65	M	1.2 (−0.08)	1.2 (−0.08)	154		153	149	185		139	45
5	56	M	0.8 (0.10)	0.9 (0.05)	398		414	417	103		118	0
6	56	F	0.15 (0.82)	0.2 (0.70)	200		228	201	72		0	0
7	65	M	0.6 (0.22)	0.9 (0.05)	278		289	278	194		122	22
8	59	M	0.8 (0.10)	0.9 (0.05)	383		389	395	106		111	67
9	59	F	1.2 (−0.08)	1.0 (0.0)	306		306	300	228		228	139
10	54	M	0.9 (0.05)	1.2 (−0.08)	490		495	483	111		51	40
11	48	M	1.2 (−0.08)	1.0 (0.0)	295		289	289	117		128	0
12	64	M	0.7 (0.15)	0.8 (0.10)	396		373	378	306		278	61
Mean	55		0.79 (0.10)	0.87 (0.06)	345		349	340	175		153	47
±SD					127		128	124	79		95	45
Photodynamic therapy												
13	58	M	0.8 (0.10)	0.7 (0.15)	390	413	385	366	368	500	369	0
14	59	M	0.15 (0.82)	0.2 (0.70)	378	451	331	289	160	345	101	0
15	56	M	0.4 (0.40)	0.5 (0.30)	641	653	592	550	91	119	94	0
16	57	M	0.3 (0.52)	0.4 (0.40)	386	487	362	375	165	387	209	0
17	70	M	0.9 (0.05)	1.2 (−0.08)	326	—	312	312	245	—	323	104
18	46	M	0.1 (1.00)	0.15 (0.82)	356	395	356	306	85	70	0	0
19	68	M	1.5 (−0.18)	1.5 (−0.18)	356	578	294	211	205	428	208	70
20	65	F	0.6 (0.22)	0.7 (0.15)	278	261	250	233	272	211	161	0
Mean	60		0.43 (0.37)	0.52 (0.27)	389	462	360	330	199	294	183	22
±SD					106	124	100	103	92	157	118	40

F = female; M = male; SD = standard deviation.
In the laser photocoagulation group, the choroidal thickness at the fovea before, 1 week after laser photocoagulation (week 1), and 4 weeks after laser photocoagulation (week 4). In the photodynamic therapy group, the choroidal thickness at the fovea before and 2 days after photodynamic therapy (day 2), 1 week after photodynamic therapy (week 1), and 4 weeks after photodynamic therapy (week 4). Choroidal thickness measured using the enhanced depth imaging spectral-domain optical coherence tomography technique. Mean best-corrected visual acuity calculated by logarithm of the minimum angle of resolution scale.

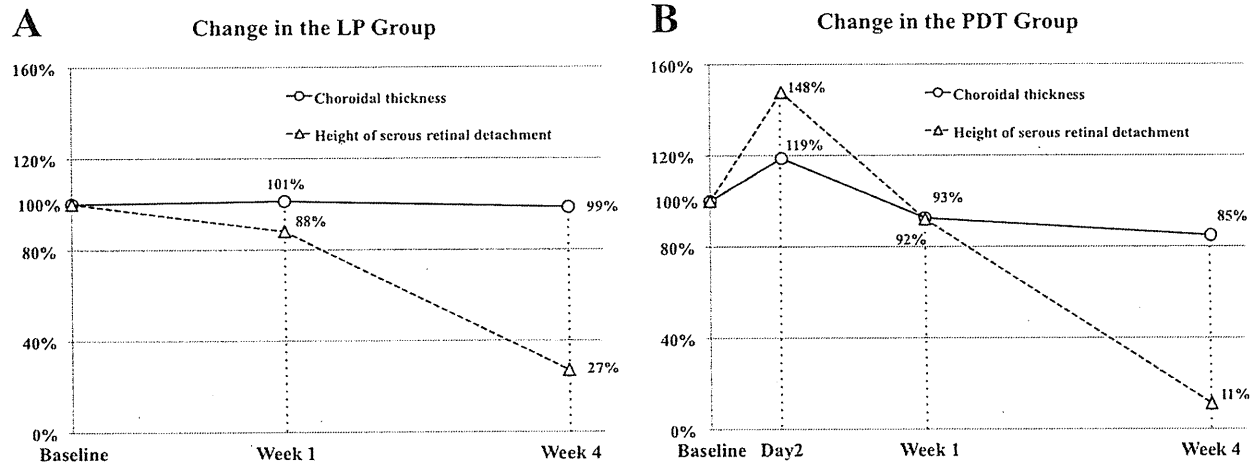

Figure 1. A, Graph showing the percentage change of the choroidal thickness and the height of serous retinal detachment after laser photocoagulation (LP) compared with baseline. Open circles with the connecting solid line indicate the change of the choroidal thickness, and open triangles with the connecting dashed line indicate the height of serous retinal detachment. The height of serous retinal detachment decreased at weeks 1 and 4, whereas the choroidal thickness remained the same. B, Graph showing the percentage change of the choroidal thickness and the height of serous retinal detachment after photodynamic therapy (PDT) compared with baseline. The patients in the PDT group were treated by half-dose verteporfin PDT. Open circles with the connecting solid line indicate the change of the choroidal thickness, and open triangles with the connecting dashed line indicate the height of serous retinal detachment. Both of them increased at day 2 and decreased at weeks 1 and 4. Baseline; before photodynamic therapy, day 2; 2 days after photodynamic therapy, week 1; 1 week after photodynamic therapy, week 4; 4 weeks after photodynamic therapy.

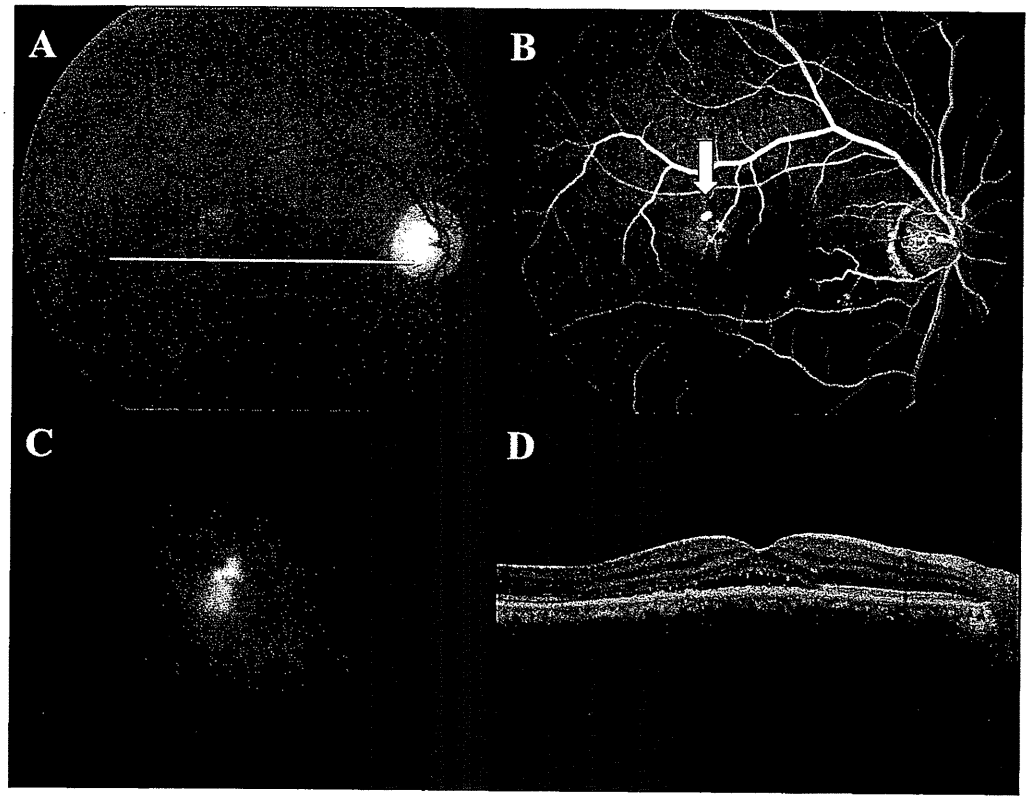

Figure 2. Case 5: a 56-year-old man noted blurred vision in the right eye. The best-corrected visual acuity at baseline was 0.80 (0.10 logarithm of the minimum angle of resolution) in the right eye. There was no history of corticosteroid treatment. A, Fundus photograph of the right eye showing a serous retinal detachment at the fovea. B, Fluorescein angiogram of the right eye showing a focal leak in the temporal macula (arrow). C, Indocyanine green angiogram from the mid phase showing a hyperfluorescent area temporally from the macula that subtended the site of focal leakage seen during fluorescein angiography. D, Optical coherence tomography image showing the serous retinal detachment at the macular area.

Patients and Methods

This study followed the tenets of the Declaration of Helsinki. The Institutional Review Board at Fukushima Medical University School of Medicine approved (1) observation using OCT for eyes with macular and retinal disorder, (2) PDT for the CSC, (3) the observational study for age-related macular degeneration and its similar disorders (including CSC) at the treatment and follow-up, and (4) the retrospective comparative analysis performed in this study.

The clinical examination for diagnosis of CSC included measurement of best-corrected visual acuity (BCVA), slit-lamp biomicroscopy with a contact lens or noncontact lens, indirect ophthalmoscopy, digital fluorescein angiography, and ICGA (TRC-50IX/IMAGEnet H1024 system; Topcon, Tokyo, Japan). The BCVA measurement with a Japanese standard decimal visual chart and the logarithm of the minimum angle of resolution (logMAR) scale were used for analysis. All eyes were examined with the Heidelberg Spectralis OCT (Heidelberg Engineering, Heidelberg, Germany). The following were inclusion criteria: (1) patients with BCVA of 0.10 (1.00 logMAR) or better, (2) patients with a serous retinal detachment involving the fovea on OCT; (3) patients with

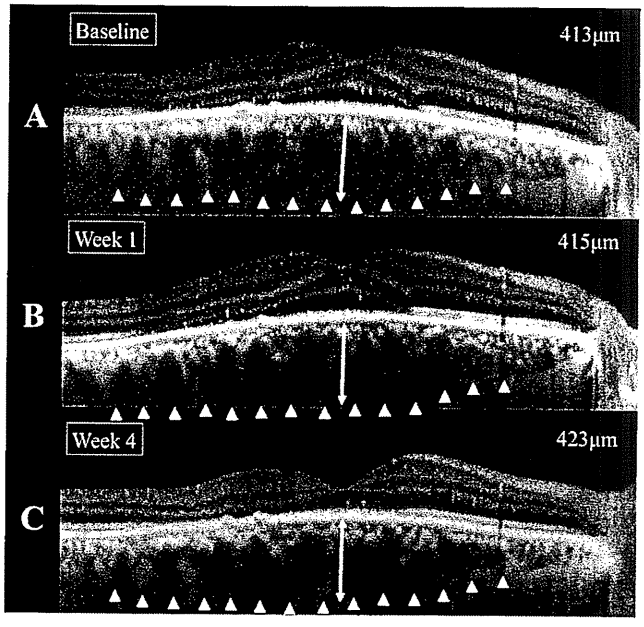

Figure 3. Enhanced depth imaging spectral-domain optical coherence tomography images from the same case as Figure 2. Laser photocoagulation was performed successfully by the following: the set for a spot size of 200 μm, power of 100 mW, and application time of 0.20 seconds. The choroidal thickness of the horizontal images at baseline was (A) 413 μm, (B) 415 μm at week 1, and (C) 423 μm at week 4. The serous retinal detachment resolved by week 4. The best-corrected visual acuity at week 4 was 0.9 (0.05 logarithm of the minimum angle of resolution). Baseline; before laser photocoagulation, week 1; 1 week after laser photocoagulation, week 4; 4 weeks after laser photocoagulation.

CSC according to the diagnostic criteria: CSC was diagnosed if patients had subretinal fluid involving the macula associated with the idiopathic leaks from the RPE during fluorescein angiography. Indocyanine green angiography was used to confirm the presence of choroidal vascular hyperpermeability, to determine the size of the hyperpermeability to guide the PDT if indicated, and to rule out the presence of polypoidal choroidal vasculopathy. Classic CSC was diagnosed if the patients had isolated points of leakage. Chronic CSC was diagnosed if the patients had widespread areas of leakage visualized as diffuse or poorly defined regions of leakage originating from broad areas of RPE damage.

Patients with classic CSC with the apparent focal leakage were treated with LP (LP group). Patients with chronic CSC without the apparent focal fluorescein leakage and with the persistent serous retinal detachment of more than 6 months' duration were treated with half-dose verteporfin PDT (PDT group). All patients had subjective visual loss, and they had the occupational needs or desired treatment after being informed of the risks and benefits. The duration of the serous retinal detachment was inferred from the patient's recall of the onset of visual symptoms.

Laser photocoagulation in the LP group was performed using a DPSS yellow laser (561 nm; Nidek, Gamagori, Japan) with a spot size of 200 μm, at a power of 70 to 100 mW, with an application time of 0.20 seconds. The end point of the LP was the production of a slight graying of the RPE. The PDT protocol for chronic CSC was performed by using the half-dose (3 mg/m^2) as compared with the normal dose (6 mg/m^2) of verteporfin (Visudine; Novartis, Switzerland) for treating CSC.[13] The verteporfin was infused over 10 minutes followed by delivery of an activating light dose of 50 J/cm^2 from a 689-nm laser system (Carl Zeiss, Dublin, CA) over an 83-second exposure time. The laser spot size for the PDT was the diameter of the region of indocyanine green hyperpermeability plus 1 mm.

The change in subfoveal choroidal thickness was observed by the EDI OCT technique,[15] in which the Heidelberg Spectralis OCT instrument is pushed in close enough to the eye to obtain an inverted image. Each section was obtained using eye tracking, and 100 scans were averaged to improve the signal-to-noise ratio. The images were reinverted for display purposes. Additional hardware or software is not necessary with the Heidelberg Spectralis OCT for the EDI OCT technique. Other devices of OCT (e.g., the 3D-OCT (Topcon Inc, Tokyo, Japan) and RTVue (Optovue Inc, Fremont, CA) have a software setting that enables the instruments to perform the equivalent of EDI OCT without having to invert the image. The choroidal thickness and the height of the retinal detachment were measured using the attached measuring software in the Heidelberg Spectralis OCT. The subfoveal choroidal thickness was measured from the outer surface of the line formed by the RPE to the inner surface of the observed sclera. The choroidal thickness was measured from a vertical and a horizontal section under the

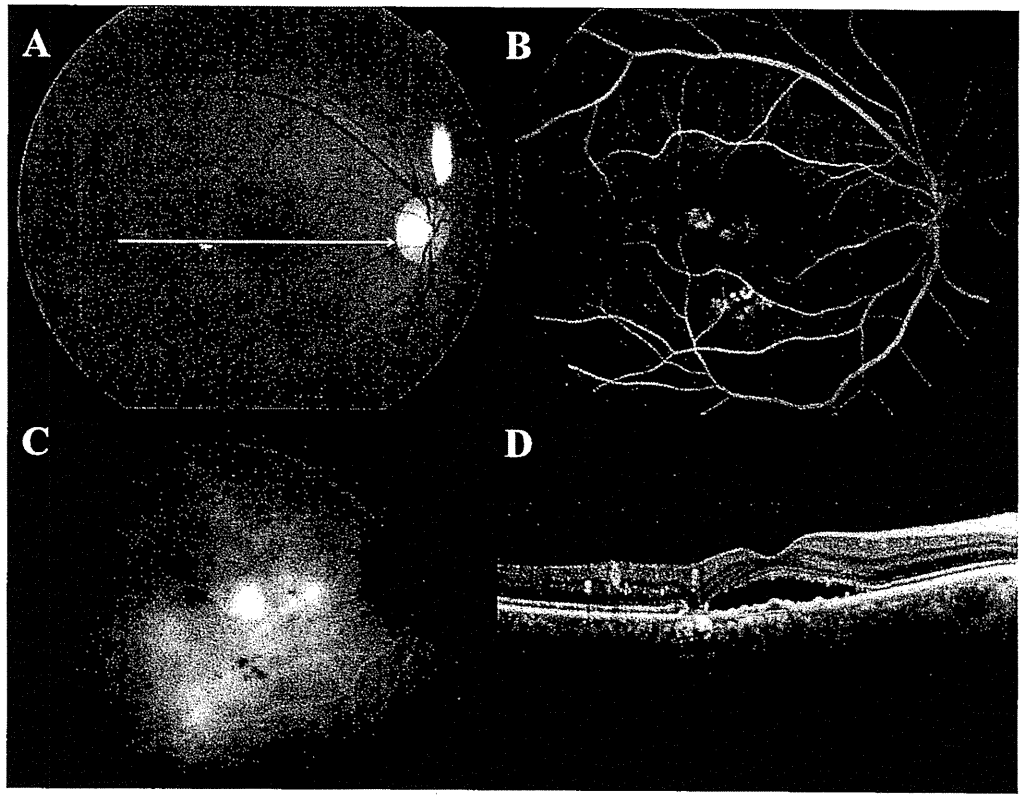

Figure 4. Case 14: a 59-year-old man reported decreased vision in his right eye resulting from the persistent subretinal fluid. He reported an episode of decreased visual acuity in the right eye 5 years previously, and he had a history of laser photocoagulation for the persistent central serous chorioretinopathy in that eye. The best-corrected visual acuity at baseline was 0.15 (0.82 logarithm of the minimum angle of resolution) in the right eye. There was no history of corticosteroid treatment. A, Fundus photograph of the right eye showing a serous retinal detachment at the center of the macular area and retinal pigment epithelial scar resulting from laser photocoagulation at the temporal area to the fovea. B, Fluorescein angiogram of the right eye showing the diffuse leakage in the central and inferior macular area. C, Indocyanine green angiogram in the mid phase showing hyperfluorescence secondary to choroidal vascular hyperpermeability in the posterior pole, including the macular area. D, Spectral-domain optical coherence tomography image showing the serous retinal detachment at the macular area, subretinal deposits at the posterior surface of the neurosensory retina, and retinal pigment epithelium irregularity.

center of the fovea from OCT data, and these were averaged. For the LP group, the subfoveal choroidal thickness was measured before LP (baseline), 1 week after LP (week 1), and 4 weeks after LP (week 4). For the PDT group, the subfoveal choroidal thickness was measured before PDT (baseline), 2 days after PDT (day 2), at week 1, and at week 4. The OCT examination was performed at all visits. In Japan, the patients who have undergone a first PDT treatment should stay in the hospital for 2 nights to avoid sun exposure. The height of retinal detachment at the fovea, measured concurrently, was defined as the distance between the outer surface of the neurosensory retina and the inner surface of the RPE. The reported measurements from OCT images represented the average of measurements made by the coauthors (IM, YS, AO), who were masked to treatment status. The visual acuities are stated as decimal equivalents and also as the logMAR equivalents. The results of the measurement of the choroidal thickness and the height of retinal detachment were analyzed using the Student *t* test.

Results

The study included 20 eyes of 20 patients. The mean age of the patients was 57.0±8.2 years, and 16 patients were male. There were 12 eyes of 12 patients with classic CSC and 8 eyes of 8 patients with chronic CSC. The mean baseline decimal visual acuity was 0.79 (0.10 logMAR) for eyes with classic CSC and 0.43 (0.37 logMAR) for those with chronic CSC. The mean number of LP spots was 5.6±2.3 and the mean treatment spot size for the PDT group was 6288±872 μm. The patients treated with both LP and PDT required only 1 treatment session, and no treatment complications were observed.

The mean subfoveal choroidal thickness and the mean height of serous retinal detachment at baseline and changes with follow-up for both groups are summarized in Table 1 and Figure 1. Figures 2 and 3 are shown as the representative case in the LP group, and Figures 4, 5, and 6 are shown as the representative case in the PDT group. All data was collected except for day 2 of case 17 in the PDT group. In the LP group, the mean choroidal thickness was 345±127 μm at baseline, 349±124 μm at week 1 ($P = 0.3$, as compared with baseline), and 340±124 μm at week 4 ($P = 0.2$, as compared with baseline). The mean choroidal thickness in the PDT group increased significantly from 389±106 μm at baseline to 462±124 μm at day 2 ($P = 0.008$) and then decreased to 360±100 μm at week 1 ($P = 0.001$, as compared with baseline) and 330±103 μm at week 4 ($P<0.001$, as compared with baseline). Nine cases in the LP group and 2 cases in the PDT group still had serous retinal detachment at week 4; however, the subretinal fluid disappeared in all cases within 2 months after treatment. The EDI OCT images at day 2 showed the hyperreflective material in the subretinal space possibly because of PDT-induced exudation from the choroid (Fig 5B). There was no similar exudation at week 1 and week 4 in EDI OCT images (Fig 5C, D). The morphologic resolution of retinal detachment tended to occur subsequent to the decrement of choroidal thickness in the PDT group. All cases of the PDT group had decreased choroidal vascular hyperpermeability during ICGA after treatment, which were confirmed by masked evaluation (Fig 6). Only one case (case 11) in the LP group underwent repeat ICGA, which showed no change in choroidal vascular hyperpermeability after LP.

The mean BCVA levels in the LP group at baseline, week 1, and week 4 were 0.79 (0.10 logMAR), 0.82 (0.09 logMAR), and 0.87 (0.06 logMAR), respectively. The mean BCVA levels in the PDT group at baseline, week 1, and week 4 were 0.43 (0.37 logMAR), 0.45 (0.34 logMAR), and 0.52 (0.27 logMAR), respectively. The mean thickness (80±28 μm) of neurosensory retina in eyes with chronic CSC was significantly thinner (112±18 μm) than that of the classic CSC group at the baseline ($P<0.001$). These differences remained during the follow-up periods (116±25 μm in the LP group at week 4 and 84±27 μm in the PDT group; $P<0.001$). There were no differences in the retinal thickness

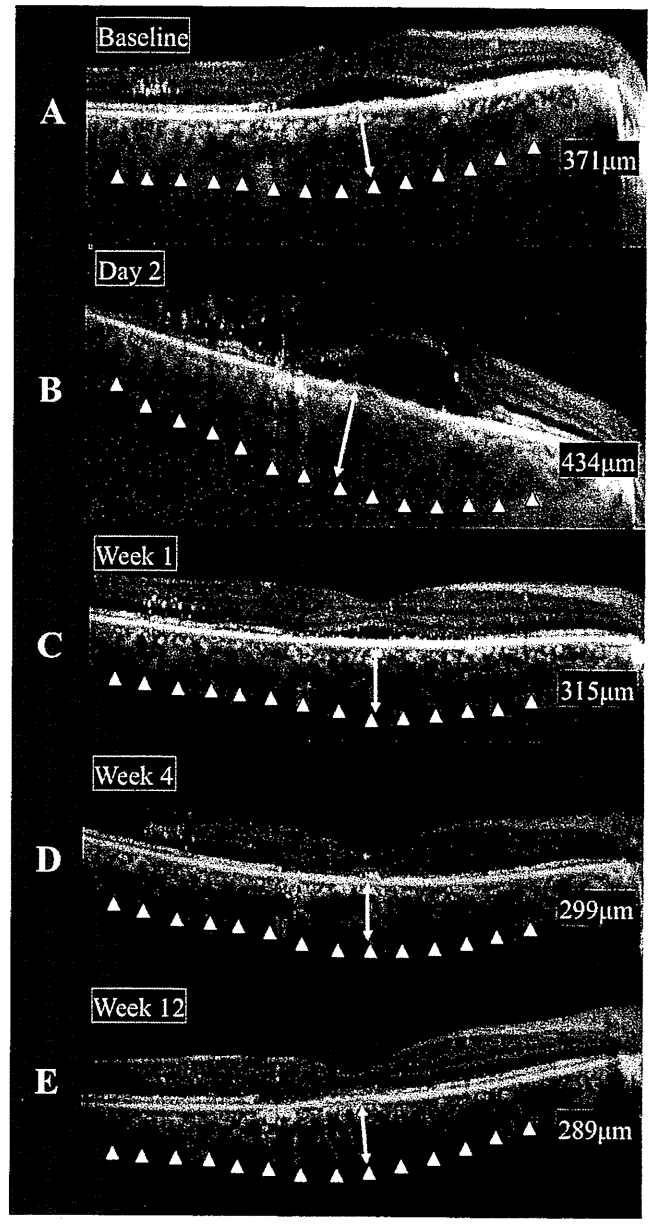

Figure 5. Enhanced depth imaging spectral-domain optical coherence tomography images from the same case as Figure 4. Half-dose verteporfin photodynamic therapy was performed successfully with the spot size of 6800 μm covering the greatest linear diameter of the hyperfluorescence in the indocyanine green angiogram with an added 1 mm. The choroidal thickness in the horizontal images at baseline was (A) 371 μm, and (B) increased to 434 μm at day 2, (C) reduced to 315 μm at week 1, (D) 299 μm at week 4, and (E) 289 μm at week 12. Optical coherence tomography images obtained on day 2 (B) show the hyperreflective materials at the subretinal space. The serous retinal detachment disappeared at week 4. The best-corrected visual acuity was 0.2 (0.70 logarithm of the minimum angle of resolution) at week 4. Baseline; before photodynamic therapy, day 2; 2 days after photodynamic therapy, week 1; 1 week after photodynamic therapy, week 4; 4 weeks after photodynamic therapy; week 12; 12 weeks after photodynamic therapy.

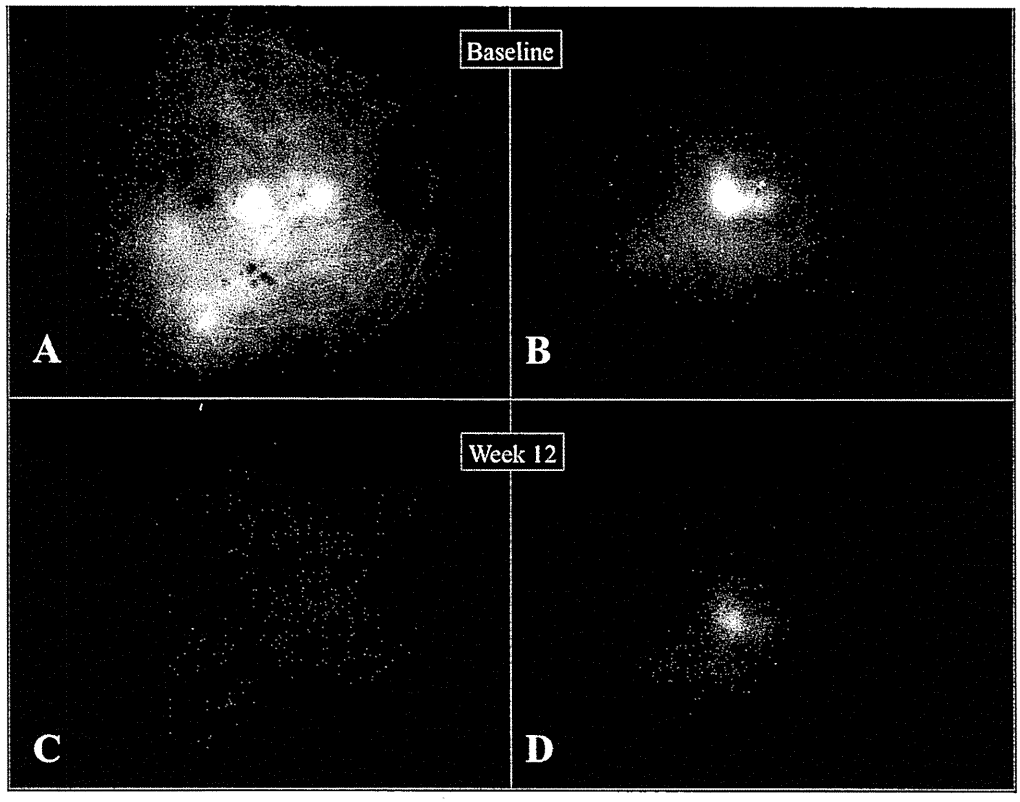

Figure 6. Indocyanine green angiograms obtained from both eyes at baseline and week 12 in the same case as Figure 4. A, B, Both eyes at baseline show the hyperfluorescence from choroidal vascular hyperpermeability at the macular area. C, D, Although the right eye at week 12 did not show hyperfluorescence, the left eye at week 12 showed the persistent hyperfluorescence at the macular area. Baseline; before photodynamic therapy; week 12; 12 weeks after photodynamic therapy.

measured at baseline as compared with week 4 ($P = 0.6$ in the LP group and $P = 0.7$ in the PDT group, respectively).

Discussion

Although there have been many theories concerning the pathogenesis of CSC, Gass[2] proposed that CSC was the result of choroidal vascular hyperpermeability. His hypothesis seemed to be confirmed by later studies that found evidence of hyperpermeability from the choriocapillaris during ICGA.[1,3–7] If there is sufficient hydrostatic pressure from choroidal vascular hyperpermeability to cause leaks from the level of the RPE and serous retinal detachment, one would expect that the choroid would be thickened as well.[16] In the present study, eyes with CSC were found to have thickened choroids. Focal LP of leaks did not result in any change in choroidal thickness, whereas PDT led to choroidal thinning and decreased hyperpermeability seen during ICGA, suggesting differing mechanisms of action for these 2 forms of treatment.

Indocyanine green angiography shows a variety of defects in CSC patients, including variable filling of regions within the choroid, choroidal venous dilation, and choroidal vascular hyperpermeability, principally arising from the choriocapillaris.[1,3–7] Central serous chorioretinopathy commonly is split into classic and chronic cases, but the underlying ICGA abnormality unifying both is choroidal vascular hyperpermeability. Indocyanine green angiographic abnormalities were found to persist after resolution of active fluorescein leakage from the level of the RPE and to be bilateral in almost all patients, although there may be signs of CSC in only 1 eye. Similarly, the choroid was found to be thickened in CSC patients as compared with controls, even in fellow eyes without active disease or in affected eyes after cessation of visible leakage.[16] Photodynamic therapy using verteporfin as a treatment for choroidal neovascularization was found to cause choriocapillaris damage and vascular remodeling in the underlying choroid.[11–14,17–21] This PDT side effect was applied to CSC in the hopes that the damage to the choroid could be used to the benefit of the patient.[11–14] Decreasing choroidal vascular hyperpermeability may decrease the exudation related to CSC.

Eyes treated with LP in the present series had a cessation of leakage without a change in choroidal thickness. In 1 case, the ICGA results after LP showed that the hyperpermeability remained the same. Past studies found that the area of hyperpermeability was larger than any focal laser treatment spots and that the choroidal vascular hyperpermeability persisted even after successful LP.[5,6] Because neither the hyperpermeability seen during ICGA nor the choroidal thickness changes, it is not likely that a widespread alteration in choroidal function was obtained by LP. As such, LP may affect the local environment around the leak.

Immediately after PDT, eyes with CSC showed signs of increased exudation. A transient increase in exudation has been seen in eyes with choroidal neovascularization treated with PDT.[21–26] Eventually, the eyes with CSC showed decreased hyperpermeability during ICGA and decreased choroidal thickness. This suggests that a more widespread alteration in choroidal function induced by PDT may explain, in part, the physiologic effects induced by PDT in CSC eyes. In addition, it also may explain the relatively low rates of recurrence of CSC after PDT[11–14]: the induced changes within the choroid caused by PDT may normalize the choroidal permeability to the extent that abnormally increased hydrostatic pressure is less likely to occur.

Optical coherence tomography can visualize structures within the eye as dictated by the wavelength range of the light source and the imaging methods used. Although the deeper penetration OCT using a 1-μm wavelength has been studied recently, OCT instruments are not commercially available.[27–30] Some authors have reported the choroidal thickness of the various diseases using the EDI OCT technique, such as age-related macular degeneration with pigment epithelial detachment,[31] CSC,[16] age-related choroidal atrophy,[32] normal eyes,[33] and highly myopic eyes.[34] This imaging technique can provide images with less apparent noise than published images using the 1-μm light source.[27–30]

This retrospective study had several limitations, including a small sample size and short-term follow-up. Additional study is needed to investigate the relationship among the extent and severity of hyperpermeability seen during ICGA and the amount of choroidal thickening. Such a study would require a much larger number of patients than was examined in the present study because of known interactions between choroidal thickness and age and also refractive error. The patients in the present study were relatively old, and younger patients need to be evaluated. Because PDT with verteporfin potentially may cause choriocapillaris damage, choroidal ischemia,[17–21] and retinal toxicity,[35] potential for visually significant side effects may be reduced by avoiding direct treatment of the fovea. Further investigations also could examine fovea-sparing PDT techniques to lessen risk of visually significant complications for patients who do not have subfoveal leaks. It may be possible to reduce choroidal vascular hyperpermeability enough to benefit the patient without having to treat the subfoveal choroid. In the present study, EDI OCT was helpful in monitoring the proposed site for the pathophysiologic changes in CSC and the choroid and provided information not available by other means.

References

1. Klais CM, Ober MD, Ciardella AP, Yannuzzi LA. Central serous chorioretinopathy. In Ryan SJ, ed-in-chief, Hinton DR, Schachat AP, Wilkinson CP, eds. Retina. 4th ed. vol. 2. Philadelphia: Elsevier Mosby; 2006;1135–61.
2. Gass JD. Pathogenesis of disciform detachment of the neuroepithelium. II. Idiopathic central serous choroidopathy. Am J Ophthalmol 1967;63:587–615.
3. Scheider A, Nasemann JE, Lund OE. Fluorescein and indocyanine green angiographies of central serous choroidopathy by scanning laser ophthalmoscopy. Am J Ophthalmol 1993; 115:50–6.
4. Guyer DR, Yannuzzi LA, Slakter JS, et al. Digital indocyanine-green videoangiography of occult choroidal neovascularization. Ophthalmology 1994;101:1727–35.
5. Piccolino FC, Borgia L. Central serous chorioretinopathy and indocyanine green angiography. Retina 1994;14:231–42.
6. Iida T, Kishi S, Hagimura N, Shimizu K. Persistent and bilateral choroidal vascular abnormalities in central serous chorioretinopathy. Retina 1999;19:508–12.
7. Spaide RF, Goldbaum M, Wong DW, et al. Serous detachment of the retina. Retina 2003;23:820–46.
8. Spaide RF, Hall L, Haas A, et al. Indocyanine green videoangiography of older patients with central serous chorioretinopathy. Retina 1996;16:203–13.
9. Ficker L, Vafidis G, While A, Leaver P. Long-term follow-up of a prospective trial of argon laser photocoagulation in the treatment of central serous retinopathy. Br J Ophthalmol 1988; 72:829–34.
10. Yap EY, Robertson DM. The long-term outcome of central serous chorioretinopathy. Arch Ophthalmol 1996;114:689–92.
11. Yannuzzi LA, Slakter JS, Gross NE, et al. Indocyanine green angiography-guided photodynamic therapy for treatment of chronic central serous chorioretinopathy: a pilot study. Retina 2003;23:288–98.
12. Cardillo Piccolino F, Eandi CM, Ventre L, et al. Photodynamic therapy for chronic central serous chorioretinopathy. Retina 2003;23:752–63.
13. Chan WM, Lai TY, Lai RY, et al. Safety enhanced photodynamic therapy for chronic central serous chorioretinopathy: one-year results of a prospective study. Retina 2008;28:85–93.
14. Chan WM, Lai TY, Lai RY, et al. Half-dose verteporfin photodynamic therapy for acute central serous chorioretinopathy: one-year results of a randomized controlled trial. Ophthalmology 2008;115:1756–65.
15. Spaide RF, Koizumi H, Pozzoni MC. Enhanced depth imaging spectral-domain optical coherence tomography. Am J Ophthalmol 2008;146:496–500.
16. Imamura Y, Fujiwara F, Margolis R, Spaide RF. Enhanced depth imaging optical coherence tomography of the choroid in central serous chorioretinopathy. Retina 2009;29:1469–73.
17. Schmidt-Erfurth U, Hasan T, Gragoudas E, et al. Vascular targeting in photodynamic occlusion of subretinal vessels. Ophthalmology 1994;101:1953–61.
18. Kramer M, Miller JW, Michaud N, et al. Liposomal benzoporphyrin derivative verteporfin photodynamic therapy: selective treatment of choroidal neovascularization in monkeys. Ophthalmology 1996;103:427–38.
19. Schmidt-Erfurth U, Laqua H, Schlötzer-Schrehard U, et al. Histopathological changes following photodynamic therapy in human eyes. Arch Ophthalmol 2002;120:835–44.
20. Schlötzer-Schrehardt U, Viestenz A, Naumann GO, et al. Dose-related structural effects of photodynamic therapy on choroidal and retinal structures of human eyes. Graefes Arch Clin Exp Ophthalmol 2002;240:748–57.
21. Isola V, Pece A, Parodi MB. Choroidal ischemia after photodynamic therapy with verteporfin for choroidal neovascularization. Am J Ophthalmol 2006;142:680–3.
22. Schmidt-Erfurth U, Michels S, Barbazetto I, Laqua H. Photodynamic effects on choroidal neovascularization and physiological choroid. Invest Ophthalmol Vis Sci 2002;43:830–41.

23. Rogers AH, Martidis A, Greenberg PB, Puliafito CA. Optical coherence tomography findings following photodynamic therapy of choroidal neovascularization. Am J Ophthalmol 2002; 134:566–76.
24. Costa RA, Farah ME, Cardillo JA, et al. Immediate indocyanine green angiography and optical coherence tomography evaluation after photodynamic therapy for subfoveal choroidal neovascularization. Retina 2003;23:159–65.
25. Schmidt-Erfurth U, Schlötzer-Schrehard U, Cursiefen C, et al. Influence of photodynamic therapy on expression of vascular endothelial growth factor (VEGF), VEGF receptor 3, and pigment epithelium-derived factor. Invest Ophthalmol Vis Sci 2003;44:4473–80.
26. Koizumi H, Iida T, Nagayama D, et al. Indocyanine green angiography in eyes with substantially increased subretinal fluid 1 week after photodynamic therapy. Retin Cases Brief Rep 2008;2:12–4.
27. Povazay B, Hofer B, Torti C, et al. Impact of enhanced resolution, speed and penetration on three-dimensional retinal optical coherence tomography. Opt Express [serial online] 2009;17:4134–50. Available at: http://www.opticsinfobase.org/abstract.cfm?URI=oe-17-5-4134. Accessed December 8, 2009.
28. Yasuno Y, Miura M, Kawana K, et al. Visualization of subretinal pigment epithelium morphologies of exudative macular diseases by high-penetration optical coherence tomography. Invest Ophthalmol Vis Sci 2009;50:405–13.
29. de Bruin DM, Burnes DL, Loewenstein J, et al. In-vivo three-dimensional imaging of neovascular age-related macular degeneration using optical frequency domain imaging at 1050 nm. Invest Ophthalmol Vis Sci 2008;49:4545–52.
30. Huber R, Adler DC, Srinivasan VJ, Fujimoto JG. Fourier domain mode locking at 1050 nm for ultra-high-speed optical coherence tomography of the human retina at 236,000 axial scans per second. Opt Lett 2007;32:2049–51.
31. Spaide RF. Enhanced depth imaging optical coherence tomography of retinal pigment epithelial detachment in age-related macular degeneration. Am J Ophthalmol 2009;147:644–52.
32. Spaide RF. Age-related choroidal atrophy. Am J Ophthalmol 2009;147:801–10.
33. Margolis R, Spaide RF. A pilot study of enhanced depth imaging optical coherence tomography of the choroid in normal eyes. Am J Ophthalmol 2009;147:811–5.
34. Fujiwara T, Imamura Y, Margolis R, et al. Enhanced depth imaging optical coherence tomography of the choroid in highly myopic eyes. Am J Ophthalmol 2009;148:445–50.
35. Paskowitz DM, Donohue-Rolfe KM, Yang H, et al. Neurotrophic factors minimize the retinal toxicity of verteporfin photodynamic therapy. Invest Ophthalmol Vis Sci 2007;48: 430–7.

Footnotes and Financial Disclosures

Originally received: August 31, 2009.
Final revision: December 31, 2009.
Accepted: January 8, 2010.
Available online: May 15, 2010. Manuscript no. 2009-1189.

[1] Department of Ophthalmology, Fukushima Medical University School of Medicine, Fukushima, Japan.

[2] Vitreous, Retina, Macula Consultants of New York, New York, New York.

Financial Disclosure(s):
The author(s) have no proprietary or commercial interest in any materials discussed in this article.

Supported in part by the Macula Foundation, New York, New York.

Correspondence:
Ichiro Maruko, MD, Department of Ophthalmology, Fukushima Medical University School of Medicine, 1 Hikarigaoka, Fukushima, Japan. E-mail: imaruko@fmu.ac.jp.

Graefes Arch Clin Exp Ophthalmol (2010) 248:361–368
DOI 10.1007/s00417-009-1276-2

RETINAL DISORDERS

Combined cases of polypoidal choroidal vasculopathy and typical age-related macular degeneration

Ichiro Maruko · Tomohiro Iida · Masaaki Saito · Dai Nagayama

Received: 23 August 2009 / Revised: 8 December 2009 / Accepted: 10 December 2009 / Published online: 14 January 2010

Abstract
Background When we classified neovascular exudative age-related macular degeneration (AMD) into three types of polypoidal choroidal vasculopathy (PCV), typical AMD, and retinal angiomatous proliferation (RAP) in our previous study, we reported 5.5% had the combined cases, such as one eye had PCV and the other eye had typical AMD. We examined the clinical characteristics of these combined cases in the current study.
Methods All cases underwent fluorescein and indocyanine green angiography (FA and ICGA) at the initial examination. All PCV cases were diagnosed definitively based on characteristic aneurysmal lesions seen on ICGA. Follow-up examinations also were conducted to determine whether polypoidal lesions had developed in the eyes with typical AMD.
Results Among 349 patients with neovascular AMD, 20 (5.7%) had one eye with PCV and the other eye with typical AMD. The average age was 73 years. The mean best-corrected visual acuity levels at the initial examination in eyes with PCV and typical AMD were 0.20 and 0.43, respectively (p=0.09). All subgroups of classic and occult CNV were observed in the eyes with typical AMD on FA. During the follow-up period (average, 21.7 months), PCV developed in ten eyes with typical AMD at the initial examination.
Conclusions Although some cases might include different stages of progression or probable cases of PCV, the combined cases in which one eye has PCV and the other eye has typical AMD suggest that those clinical entities are not independent and possibly overlap.

I. Maruko (✉) · T. Iida · M. Saito · D. Nagayama
Department of Ophthalmology,
Fukushima Medical University School of Medicine,
1 Hikarigaoka,
Fukushima 960-1247, Japan
e-mail: imaruko@fmu.ac.jp

Keywords Polypoidal choroidal vasculopathy · Age-related macular degeneration

Introduction

Neovascular exudative age-related macular degeneration (AMD) is a leading cause of legal blindness in elderly patients in developed countries. In Japan, fewer patients have neovascular AMD compared to Western countries [8, 9, 14, 17, 20]. However, the prevalence of AMD in Japan is increasing rapidly [15], and the demographic features differ from those in other countries.

We classified neovascular AMD in Japanese patients into three types and reported that among 289 patients, 158 (54.7%) were diagnosed with polypoidal choroidal vasculopathy (PCV), 102 (35.3%) with typical AMD, and 13 (4.5%) with retinal angiomatous proliferation (RAP) [13]. We concluded that neovascular AMD in Japanese patients has demographic features that differ from those in Caucasian patients. Each type is characterized by differences in clinical behavior, examination findings, and pathologic deductions. Accurate diagnoses of these types are important for appropriate patient management [2, 19]. However, we also reported that 16 patients (5.5%) had a combination of types, i.e., one eye had PCV and the other eye had typical AMD. These combined cases might indicate that these pathologies are not independent of each other. Because the proportion of PCV in neovascular AMD in Japan is more than 50%, cases with both PCV and typical AMD might be observed frequently.

In the current study, we examined the clinical characteristics of cases in which one eye had PCV and the other eye had typical AMD.

Patients and methods

The study followed the tenets of the Declaration of Helsinki. We retrospectively reviewed the medical records of the patients and there were no confidentiality issues. The institutional review board at Fukushima Medical University School of Medicine approved this retrospective analysis. All subjects provided written informed consent after the nature and possible consequences of the study were explained.

The patients with neovascular AMD in whom one eye had PCV and the other eye had typical AMD were evaluated retrospectively based on age, gender, and best-corrected visual acuity (BCVA) in each eye. The BCVA was measured with a Japanese standard decimal VA chart, and the mean BCVA was calculated using the logarithm of the minimum angle of resolution (logMAR) scale. The clinical examination included indirect ophthalmoscopy, slit-lamp biomicroscopy with a contact lens, or noncontact lens (e.g., 60 diopters), and color and red-free fundus photography. All participants were examined by digital fluorescein angiography (FA) and indocyanine green angiography (ICGA) at the initial examination. We used a digital imaging system with an infrared camera and standard fundus camera (TRC-50 IX/IMAGEnet H1024 system, Topcon, Tokyo, Japan) and a confocal laser scanning system (HRA-2, Heidelberg Engineering, Dossenheim, Germany). All angiograms were evaluated by three retina specialists (I.M., T.I., M.S.) masked to the clinical findings. We measured the lesion area in eyes with PCV and typical AMD on the FA images using IMAGENet 2000 software (Topcon). The lesion area was defined as the area of leakage caused by neovascularization and features obscuring the boundaries, including blocked fluorescence due to blood, thick exudate, hypertrophic retinal pigment epithelium (RPE), and associated pigment epithelial detachment (PED) on FA. The lesion area was measured in disc areas (DA), with one DA calculated as 2.54 mm^2 based on a standard disc diameter of 1.8 mm [1, 18]. All cases were observed by optical coherence tomography (OCT) to confirm RPE elevation and retinal morphologic changes. The following definitions were used to describe the related clinical and angiographic abnormalities evaluated in the current study.

The diagnostic criteria for PCV in the current study were proposed based on ICGA findings, which visualized the characteristic aneurysmal lesions. The Japanese Study Group of Polypoidal Choroidal Vasculopathy [7] defined the following criteria: protruded orange-red elevated lesions (excluding PED, choroidal hemangioma, and subretinal blood) observed by fundus examination and characteristic aneurysmal lesions seen on ICGA. However, only definitive cases of PCV on ICGA were included in the current study for unequivocal diagnosis. All patients with PCV were diagnosed as having neovascular AMD on FA, and then it was identified as PCV on ICGA.

The typical AMD lesion area was comprised of classic choroidal neovascularization (CNV) on FA and defined as follows: predominantly classic CNV, neovascular lesions in which the classic CNV component was greater than 50% of the total lesion area; minimally classic CNV, lesions in which the classic CNV components were less than 50% of the total lesion area; and occult CNV with no classic CNV component [2, 18]. Patients with other macular diseases such as high myopia, angioid streaks, and central serous chorioretinopathy were excluded.

All participants were examined and evaluated clinically by digital FA, ICGA, and OCT during the follow-up examinations. If polypoidal lesions developed in the eyes with typical AMD, we specified the location at which a polypoidal lesion developed during the follow-up period.

The results of a comparison of BCVA and the lesion area between the eyes with PCV and the fellow eye with typical AMD were analyzed using the Student's *t*-test. $p<0.05$ was considered significant.

Results

Among 349 patients with neovascular AMD examined between 2003 and 2005 at Fukushima Medical University Hospital, Fukushima, Japan, 20 patients (5.7%) in whom PCV was present in one eye and typical AMD in the fellow eye at the initial examination were included (16 men, four women; average age, 73 years). All patients were newly diagnosed with bilateral neovascular AMD. Although the combined cases should be defined as those in which each eye had a different type of neovascular AMD (i.e., PCV, typical AMD, or RAP), there were no cases with PCV and RAP or with typical AMD and RAP. Sixteen of the 20 patients had been included in our previous report [7]. Imaging procedures were performed successfully for all patients.

Table 1 shows the characteristics of the combined cases of PCV and typical AMD in the current study. The mean BCVA levels at the initial examination in eyes with PCV and typical AMD were 0.20 (0.71 logMAR) and 0.43 (0.37 logMAR) ($p=0.09$), respectively. The eyes with typical AMD were classified as one eye with predominantly classic CNV, five eyes with minimally classic CNV, and 14 eyes with occult with no classic CNV on FA. All subgroups classified according to classic CNV component on FA were observed in the eyes with typical AMD. The mean lesion area (DA) in eyes with PCV was larger than in eyes with typical AMD (10.8±9.2 and 5.9±3.9, respectively; $p=0.03$).

The 20 patients in the current study also underwent follow-up examinations after the initial examination (average follow-up period, 21.7 months; range, 2–48 months). In 20

Table 1 Clinical characteristics of combined cases in which one eye has PCV and the other eye has typical AMD

Patient no.	Sex	Age	Eyes with PCV			Eyes with Typical AMD					F/U (mo)
			Eye	BCVA at baseline	Lesion area (DA)	Eye	BCVA at baseline	Lesion area (DA)	Subgroup[a] on FA	develop PCV†	
1	M	76	OD	0.07	25.7	OS	0.3	5.8	ON	Yes	48
2	M	68	OD	0.8	10.6	OS	0.1	9.6	ON	Yes	6
3	M	62	OS	0.5	6.6	OD	0.5	3.0	ON	Yes	30
4	M	72	OD	0.5	11.2	OS	1.5	10.8	ON	Yes	6
5	M	75	OD	0.2	5.9	OS	0.7	2.5	ON	Yes	18
6	M	70	OD	0.02	7.9	OS	0.15	15.9	MC	Yes	30
7	M	82	OS	0.09	5.2	OD	0.04	6.1	MC	Yes	18
8	F	67	OS	0.06	11.8	OD	0.1	6.4	MC	Yes	2
9	M	79	OS	1.2	1.0	OD	0.3	8.1	MC	Yes	36
10	M	83	OD	0.1	3.7	OS	1.5	1.3	MC	Yes	30
Mean (1–10)		74		0.19	9.0±6.8		0.24	7.0±4.4			21.6
11	M	67	OS	0.03	29.4	OD	0.2	7.9	ON	No	18
12	M	75	OD	0.1	9.0	OS	0.4	4.4	ON	No	36
13	M	75	OS	1.2	2.2	OD	0.2	2.6	ON	No	30
14	M	75	OS	0.5	2.8	OD	0.9	1.5	ON	No	30
15	F	81	OS	0.1	27.2	OD	0.7	3.4	ON	No	24
16	F	53	OS	1.5	6.0	OD	1.2	3.2	ON	No	18
17	M	82	OS	0.05	19.7	OD	1.2	11.5	ON	No	6
18	M	82	OS	0.04	23.6	OD	0.7	3.4	ON	No	18
19	M	71	OD	0.3	3.9	OS	1.0	2.5	ON	No	6
20	F	66	OS	1.2	2.0	OD	1.0	7.2	PC	No	24
Mean (11–20)		73		0.18	12.6±11.1		0.60	4.8±3.1			20.7
Mean all		73		0.20	10.8±9.2		0.43	5.9±3.9			21.7

PCV = polypoidal choroidal vasculopathy; OS = left eye; OS = right eye;

AMD = age-related macular degeneration;

BCVA = best-corrected visual acuity. Mean BCVA was calculated using the logarithm of the minimum angle of resolution (logMAR) scale

Lesion area (DA) = the lesion size (DA) of eyes with PCV and typical AMD was measured from fluorescein and Indocyanine green angiography

DA = disc area

One DA = 2.54 mm^2 based on a standard disc diameter (DD) of 1.8 mm

FA = fluorescein angiography

MC = Minimally classic CNV

ON = Occult with no classic CNV

PC = Predominantly classic CNV

CNV = choroidal neovascularization

F/U (mo) = duration of follow-up period (months)

[a] The area of the lesion of typical AMD was composed of classic choroidal neovascularization (CNV) on fluorescein angiography and evaluated as follows:

predominantly classic CNV: a neovascular lesion in which the classic CNV component was greater than 50% of the total lesion size;

minimally classic CNV: lesions in which the classic CNV components were less than 50% of the total lesion size;

occult with no classic CNV: lesions in which there was no classic CNV component.

†develop PCV = development of PCV; The PCV cases appear the polypoidal lesion in the eyes with typical AMD during the follow-up period.

eyes with typical AMD diagnosed at the initial examination, PCV developed angiographically and clinically in ten eyes during the follow-up period (Table 1). Eight of 20 eyes with typical AMD diagnosed at the initial examination underwent photodynamic therapy (PDT) or laser photocoagulation during the follow-up period. Among the eyes with typical AMD, PCV was observed in four of eight treated eyes and six of 12 untreated eyes in the eyes at the initial examination.

There was no significant difference due to therapy in development of PCV among the eyes with typical AMD at the initial examination. A polypoidal lesion on ICGA developed from the edge of the original CNV at the initial examination in seven eyes and emerged from the area within the original CNV at the initial examination in three eyes.

Case reports

Case 1 was that of a 67-year-old man (patient 11) who reported visual loss in the left eye a few years previously and acute visual loss in the right eye. The BCVA at the initial examination was 0.2 (0.70 logMAR) in the right eye

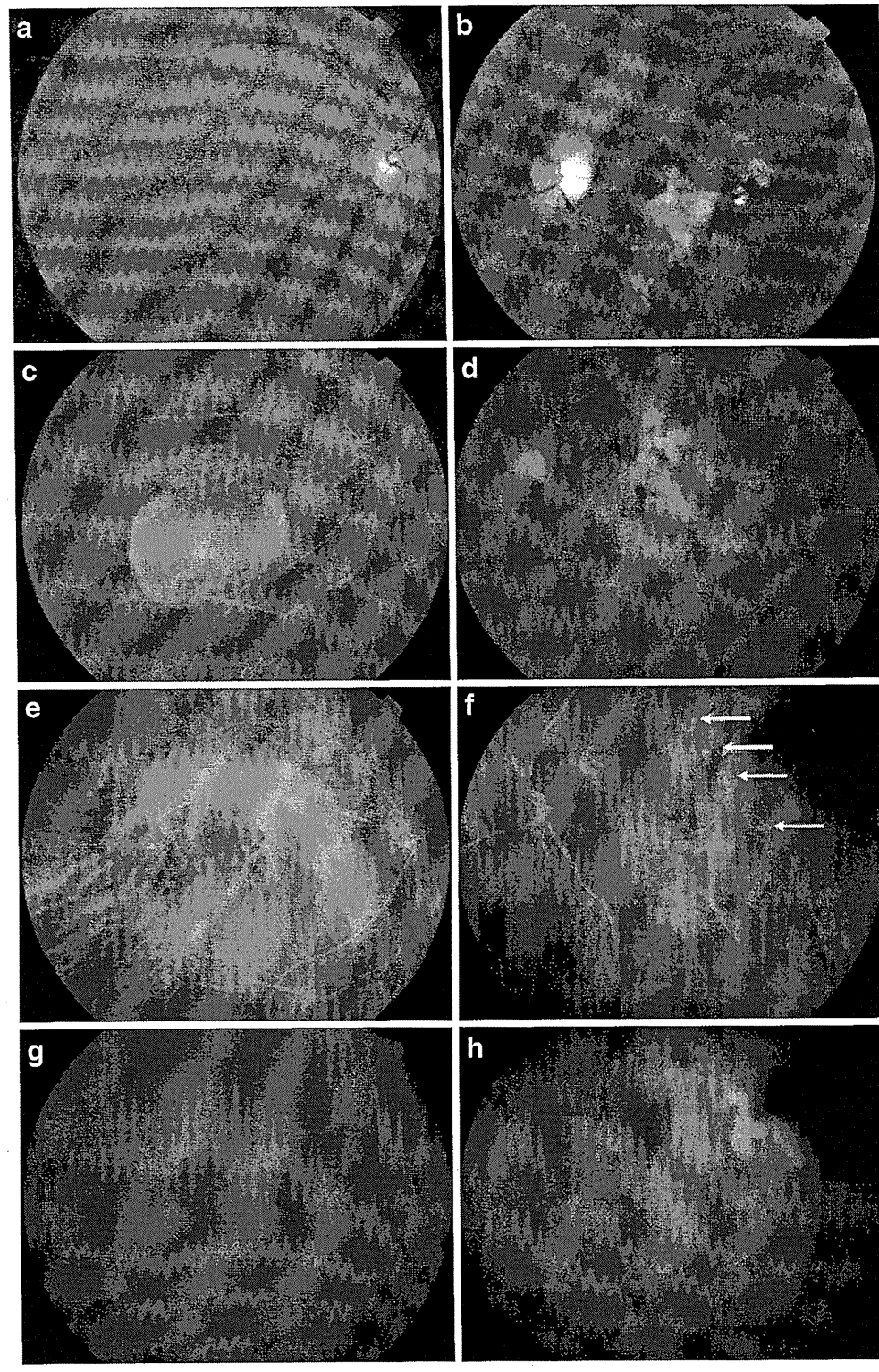

Fig. 1 Case 1 (patient 11). A 67-year-old man is representative of the combined cases of PCV and AMD in which the right eye has occult with no classic CNV and left eye has PCV. **a**, **b** A red-free fundus photograph showing RPE degeneration with a large PED in the right eye and an extensive exudative lesion with hard exudates and subretinal hemorrhage in the left eye. **c**, **d** FA shows occult CNV that includes the fovea with a large PED at the inferior fovea in the right eye and occult CNV with large fibrovascular PED in the left eye. Early phase (**e**, **f**) and late-phase (**g**, **h**) ICGA images showing hyperfluorescence corresponding to the PED in the right eye and a polypoidal lesion (*arrows*) at the superior temporal fovea in the left eye. There is no evidence of PCV in the right eye during early and late-phase ICGA

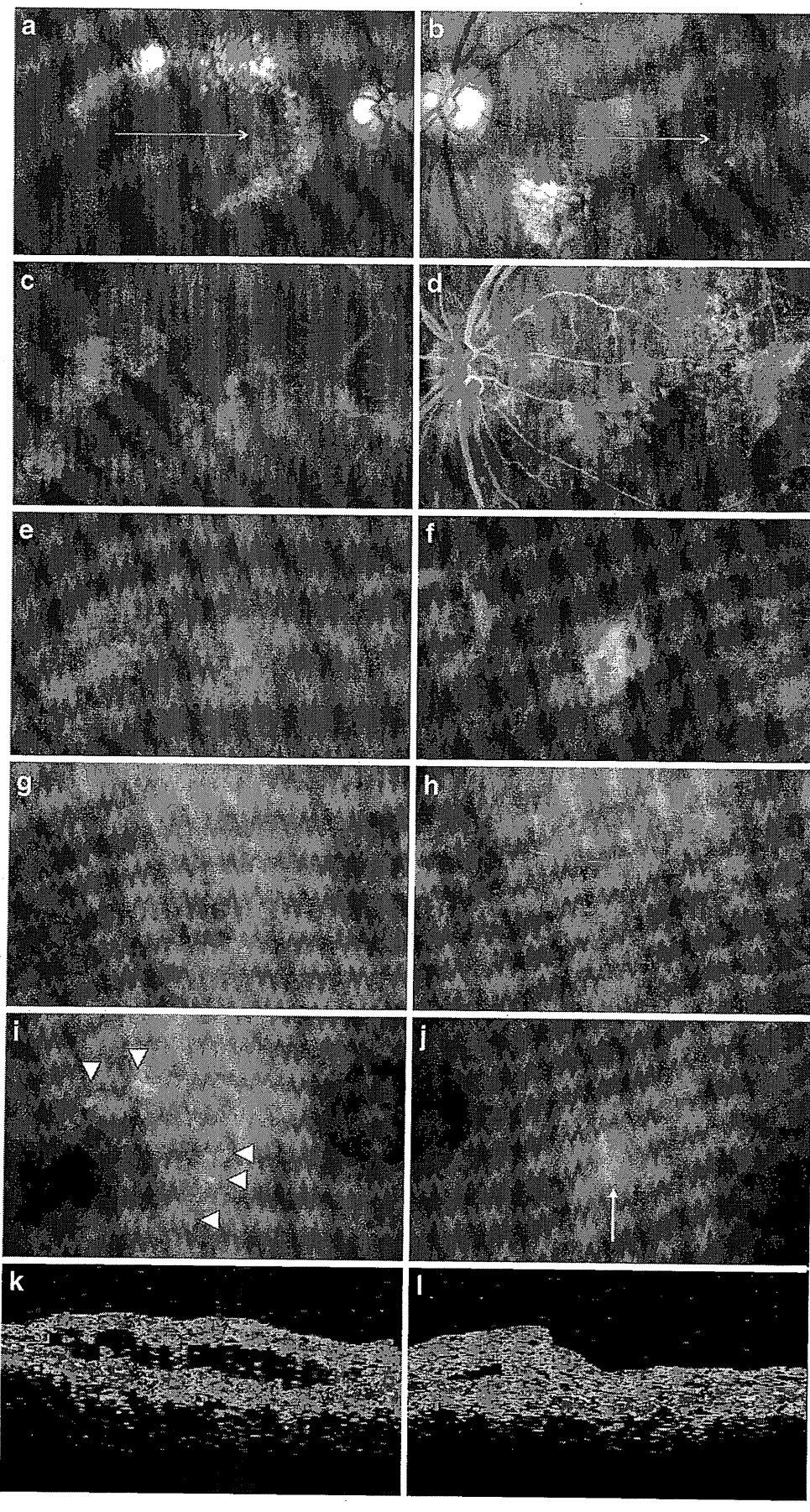

Fig. 2 Case 2 (patient 6). A 70-year-old man is representative of a combined case in which the right eye has PCV and the left eye has minimally classic CNV at the initial examination. **a**, **b** A red-free fundus photograph showing a gray-green lesion in the macular area surrounded by circinate exudates in the right eye and an extensive exudative lesion with a subretinal hemorrhage in the left eye. Early phase (**c**, **d**) and late-phase (**e**, **f**) FA images show minimally classic CNV nasal to the fovea bilaterally. Early phase (**g**, **h**) and late-phase (**i**, **j**) ICGA images show polypoidal lesions (*arrowhead*) at the outside edge of the area corresponding to the occult CNV on FA in the right eye and hyperfluorescence (*arrow*) nasal to the fovea in the left eye, which is the same area of classic CNV component on FA. There is no evidence of PCV in the left eye at the initial examination. OCT shows a serous retinal detachment in the right eye (**k**) and the hyperreflective tissue without RPE elevation at the gray-green lesion in the left eye (**l**). OCT images correspond to *horizontal white line* of (a) and (b)

and 0.03 (1.52 logMAR) in the left eye. There was RPE degeneration with a large PED in the right eye and an extensive exudative lesion with hard exudates and subretinal hemorrhages in the left eye. FA showed occult CNV that included the fovea with a large PED at the inferior fovea in the right eye and occult CNV with a large fibrovascular PED in the left eye. ICGA showed a polypoidal lesion at the superior temporal area of the fovea in the left eye. The lesion areas (DA) in eyes with typical AMD (right eye) and PCV (left eye) were 7.9 and 29.4, respectively. Although it was possible that PCV could develop in the future, there was no evidence of PCV in the right eye during the follow-up period (18 months). In this combined case of PCV and AMD, the right eye had occult CNV and the left eye had PCV (Fig. 1).

Case 2 was that of a 70-year-old man (patient 6) who had visual loss in the right eye a few years previously and sudden visual loss in the left eye. The BCVA at the initial examination was 0.15 (0.82 logMAR) in the right eye and 0.02 (1.70 logMAR) in the left eye. There was an elevated orange-red lesion in the macular area surrounded by circinate exudates in the right eye and an extensive exudative lesion that was partially gray-green with a subretinal hemorrhage in the left eye. FA showed minimally classic CNV; classic CNV was nasal to the fovea surrounded by occult CNV bilaterally. ICGA showed polypoidal lesions at the marginal edge of the area corresponding to the occult CNV on FA in the right eye. OCT showed a serous retinal detachment in the right eye and hyperreflective tissue without elevated RPE, indicating type 2 CNV above the RPE at the gray-green lesion in the left eye. There was no evidence of PCV in the left eye at the initial examination. The lesion areas (DA) in the right eye with PCV and the left eye with typical AMD were 15.9 and 7.9, respectively. In this combined case of PCV and AMD, the right eye had PCV and left eye had the minimally classic CNV of typical AMD at the initial examination. Although there was no leakage from the classic CNV in the left eye on FA after two applications of PDT, a polypoidal lesion was seen after 2.5 years on ICGA temporal to the fovea and separate from the original classic CNV. OCT temporal to the fovea in the left eye showed an elevated dome-shaped RPE corresponding to a polypoidal lesion on ICGA. PCV developed bilaterally during the 30-month follow-up period (Figs. 2 and 3).

Discussion

The current study showed that combined cases of PCV and typical AMD can develop in patients with neovascular AMD, in which one eye has PCV and the other eye has typical AMD. We identified these combined cases in 5.7% of the patients with neovascular AMD. Fifty percent of cases with typical AMD at the initial examination had a polypoidal lesion on ICGA during the follow-up period despite PDT or

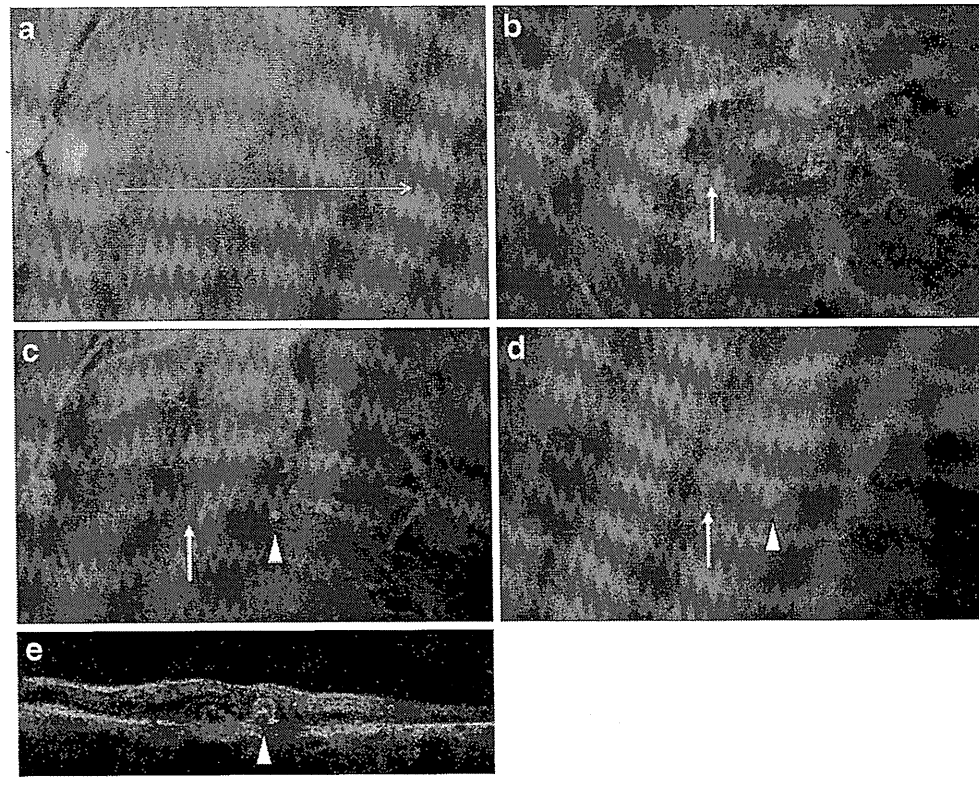

Fig. 3 Case 2. PCV in the left eye 2.5 years later in the same patient as in Fig. 2. **a** A red-free fundus photograph showing a gray-green lesion in the macular area without exudative lesion and subretinal hemorrhage. **b** FA shows no classic CNV. Early phase (**c**) and late-phase (**d**) ICGA images showing a polypoidal lesion (*arrowheads*) temporal to the fovea. *Arrows* in (b), (c), and (d) indicate the area corresponding to the classic CNV component on FA in the left eye in Fig. 2. **e** An OCT image temporal to the fovea in the left eye shows a dome-shaped RPE elevation (arrowhead) corresponding to a polypoidal lesion on ICGA. The OCT image corresponds to the horizontal white line in (a)